Pelvic joint scaling relationships and sacral shape in hominoid primates

Ingrid Lundeen

Winter 2015

Introduction

Understanding relationships between joints allows inferences to be made about the relative importance of that joint in locomotion. For example, through evolutionary time, there is an overall increase in size of the hind limb joints relative to forelimb joints of bipedal hominins (Jungers, 1988, 1991). These greater hindlimb joint sizes are thought to reflect the higher loading they must bear as posture gradually shifts to rely more on hindlimbs in propulsion, as well as increases in body size through hominin evolution. The first sacral body cross-sectional area in hominins is considered to have expanded over time in response to the higher forces inferred to have been applied by frequent bipedalality and larger body size (Abitbol, 1987; Jungers, 1988; Sanders, 1995; Ruff, 2010). Similarly, the femoral head and acetabular height have increased in size in response to an increase in body during hominin evolution (Ruff, 1988; Jungers, 1991). However, the sacroiliac joint, the intermediate joint between these two force transmission sites, has been less frequently discussed in this evolutionary context (Sanders, 1995).

The sacroiliac joint (SIJ) is a synovial, C-shaped joint where the lateral edge of the sacrum and medial edge of the ilium meet. The surface of the SIJ is lined with thick hyaline cartilage on the sacral surface and thin fibrocartilage on the iliac surface (Willard, 2007). The joint is surrounded on all sides by a capsule of strong ligaments bracing the bones against applied forces. At birth, the surface of the SIJ is

flat and smooth but changes after puberty to form slight bumps and grooves that characterize the adult SIJ (Bowen and Cassidy, 1981). These are complimentary surfaces on the sacrum and ilium that create an interlocking structure that helps resist the shock and shear stresses that act on the SIJ during high impact activities, which for humans include locomotor behaviors such as running and jumping (Vleeming et al., 1990). Despite the stabilizing benefit of developing an interlocking structure, this joint is relative flat, which allows for better transmission of forces between the bones (Vleeming and Stoeckart, 2007). The change in shape throughout growth contributes to its stability and limits the range of movement of the joint (Simonian et al., 1994).

Both the first sacral body area and femoral head diameter are frequently used to estimate body mass through the assumption that hind limb joints and proportions in orthograde primates will more accurately predict body mass than upper limb proportions (Jungers, 1988; Sanders, 1995; Ruff, 2003). The auricular surface has rarely been used to estimate body mass but due to its role in force transmission from the torso to the lower limb, it seems reasonable to link this joint to body mass, habitual posture, and movement (Jungers, 1988; Sanders, 1995). **The first goal of this study is to determine if there is a strong predictive relationship between auricular surface area and body mass in extant primates. If a strong relationship exists, this joint would represent a new joint surface that could be used to estimate body mass in fossil hominoids.**

Understanding the relationship between auricular surface area and body mass allows comparisons between other joints in the pelvis and a better understanding of the scaling relationships in primate pelves. Differences in loading patterns can indicate differences in locomotion or posture. Understanding these loading conditions in extant taxa allows for inferences regarding locomotor or postural behavior in fossil taxa. **Thus the second goal of this study is to assess the scaling relationships between the more studied joints of the pelvis, namely the acetabulum and the first sacral body, and the sacroiliac joint**.

It has been noted that sacral width gradually increases over time among bipedal fossil hominins, presumably to position the sacroiliac joints more directly over the hips and reduce stresses in the pelvis (Aiello and Dean, 1990; Lovejoy, 2005a). However, differences in the width of each individual sacral element within the sacrum have not been examined. The lower sacral elements serve as the origin of the piriformis muscle, a lateral rotator used in bipedal progression (Correa et al., 2010). A reduction in the distance between the origin and insertion of this muscle might be advantageous during bipedal progression by helping to stabilize the trunk .If this is case, one would predict relatively wider caudal sacral elements in more bipedal primates. **A third goal of this study is thus to quantify the amount of tapering in the sacrum among successive elements, in order to determine if bipeds, especially more committed forms, have relatively wide caudal sacral elements.**

Overview of Fossil Taxa in this Study

Australopithecus sp.

AL-288-1, Lucy, is a female *Australopithecus afarensis* individual from the Hadar formation in Ethiopia. This specimen, dated at 3.18 Ma (Johanson et al., 1987; Kimbel et al., 1994), preserves a complete sacrum that has suffered postmortem flattening (Johanson et al., 1987). This flattening does not appear to have affected any of the articular surfaces and only has affected the curvature of the sacrum (Sanders, 1995). In this specimen, the alar width of the sacrum relative to the width and overall size of the S1 centrum is wider than other hominoids (Haile-Selassie, 2010). Al-288-1 is unique in its large width because in general, australopith sacra are notable in terms of the relatively small size of the sacrum (Aiello and Dean, 1990). While this relatively small sacral size could be interpreted as a reflection of smaller forces applied to the joints during a form of locomotion different than any we see in modern humans, Haeusler (2002) points out the similarity in the size of the sacral bodies of *Pan* and *H. sapiens* despite differences in locomotion which suggests that sacral body area is not reflective of locomotion alone.

Australopithecus africanus sacral anatomy is best represented by Sts 14 and STW 431. Both of these specimens are associated with enough post-cranial and dental material to reliably associate them with the species. Sts 14 is reported to be a female individual from the Sterkfontein cave site, which is dated to 2.5 ma (Robinson, 1972; Sanders, 1995; Ruff, 2010). The sacrum associated with this individual preserves the first two sacral elements with the right ala missing, but

reconstructed. This individual is noted to be small in absolute size relative to extant great apes and has an auricular surface that barely extends onto the second sacral vertebra (Robinson, 1972). STW 431 is a male *Au. africanus* that is also from Sterkfontein and dated at 2.5 Ma (Tobias, 1987; Toussaint et al., 2003; Ruff, 2010). This individual preserves the first three sacral elements and although the right lateral edge of the S2 and S3 are missing, the left auricular surface is mostly preserved (Toussaint et al., 2003). Both of these *Au. africanus* sacra preserve very robust alae indicating well-developed SIJ ligaments which would imply a need for reinforcement at this joint in this species (Haeusler, 2002).

Australopithecus sediba is represented by two reconstructed pelves, MH1 and MH2. These specimens have wide iliac tuberosities and anterioposteriorly wide sacral alae – similar to the conditions in STW 431 (Toussaint et al., 2003). MH2 is distinctive in having a feature that had previously only been seen on STW 431 and modern humans – an auricular surface that extends to the third sacral vertebra (Kibii et al., 2011). The size of the iliac tuberosity and the large size of the dorsal sacral tuberosity both indicate large attachment sites for the interosseous and short posterior sacroiliac ligaments – aspects which Kibbii et al. (2011) and Simpson et al. (2008) both describe as typical *Homo* traits, but are seen to some degree in *Au sediba* (Kibbii et al., 2011), *Au africanus* (Haeusler, 2002), and *Au afarensis* (Haile-Selassie et al., 2010). The *Au. sediba* pelvic and sacral remains are reconstructed and were excluded from the metric portion of this study, however, they are included in discussion as they preserve features that are typically seen in modern humans such

as an extended auricular surface and strong ligament attachment sites (Toussaint et al., 2003).

Homo sp.

In 2008, Simpson and colleagues published a new and nearly complete hominin pelvis, BSN49/P27 that is significant for a few reasons. These researchers attributed the pelvis to a female *H. erectus*; if this attribution is correct, it is the most complete pelvis of its kind. Furthermore, it is dated to between 0.9-1.4 Ma, filling in a large gap between AL 288-1 at 3.18 Ma and the Atapuerca 1 pelvis from Spain at 0.6 Ma (Simpson et al., 2008, 2014). This individual is also significant because it exhibits a diversity of traits causing some researchers to believe it to be attributable to a different, contemporary hominin taxon, *Paranthropus boisei* (Ruff, 2010). These traits include an acetabular diameter that falls within the range of those of australopiths and an estimated body mass (33.2kg), that, if attributable to *Homo erectus*, would imply a larger degree of sexual dimorphism for *H. erectus* than observed in any living primate species (Ruff, 2010). However, Simpson and colleagues (2014) point out that this time period is particularly problematic for inferring taxonomic identity from body size because there is a lot of size variation in *Homo* individuals at this time period. Even within a single site, large amounts of body size variation have been observed (Lordkipanadze et al., 2007).

BSN49/P27 was noted to be female on the basis of a wide greater sciatic notch and subpubic angle, everted ischia, rectangular pubic bodies with a ventral

arc, subpubic concavity, large sacral angle, nonprojecting sacral promontory, and preauricular sulcus (Simpson et al., 2008). If female, this pelvis could potentially reveal much about the change in female pelvic shape as it relates to ability to birth larger infants and thus have implications for estimated postnatal growth in *Homo erectus* (Aiello and Dean, 1990). Previous discussions regarding birth canal size and postnatal growth in *H. erectus* have been based on female pelvic estimates obtained through examination of the juvenile male KNM-WT 15000 (Ruff and Walker, 1993; Bramble and Lieberman, 2004). These estimates have suggested that this species had a relatively narrow birth canal and therefore gave birth to developmentally immature offspring, as in modern humans (Walker and Ruff, 1993). However, estimates of the birth canal size derived from the BSN49/P27 pelvis suggest a larger birth canal, thus a modestly larger neonate head size (315ml; Simpson et al., 2008) than previously estimated for *Homo erectus*.

BSN49/P27 has an expanded retroauricular area, indicating extremely strong interosseous sacroiliac ligament attachments. There are also primitive traits preserved in this specimen including a relatively small auricular surface area and a sacrum that is relatively narrow in superior view (Simpson et al., 2008). Due to its recent discovery, few studies have included this individual but the diversity of traits listed above indicates the need for further investigation into its taxonomic identity and functional significance.

KNM-ER 3228 is a male *Homo erectus* individual from a site in East Turkana, Kenya dated at 1.9 Ma (Rose, 1984). This individual preserves an ilium with both

acetabulum and auricular surface but lacks a sacrum (Rose, 1984). This individual has a number of primitive features including a laterally diverging iliac blade that is wide in the sagittal plane, a small auricular surface, and a protuberant anterior superior iliac spine (Rose, 1984). However the pelvis has a number of *H. erectus* features including deep fossa on the gluteal surface of the ilium, relatively shallow iliac fossa, and extensive iliac tuberosity (Rose, 1984).

KNM-WT 15000, *H. erectus*, was not included in this study as it is a juvenile (Brown et al., 1983) and this study aimed to assess the condition of the sacrum in adult hominoids.

SH1, *Homo heidelbergensis*, is a nearly complete pelvis from Sima de los Huesos that preserves most of the ilia, included the auricular surface, and a partial sacrum (Arsuaga et al., 1999). The sacrum, although complete in length is broken on its lateral margins in the last three elements and has been noted to display extensive bone remodelling on the preserved lateral margins, with the exception of the auricular surfaces (Bonmati et al., 2010). Much of the fossil pelvic material from Sima de los Huesos, including this specimen, is described as sharing features, such as pronounced iliac flare and protruding acetabular roof, with earlier *Homo* such as KNM-ER 3228 (Arsuaga et al., 1999; Bonmati et al., 2010). This adult individual has been sexed as male due to the extreme robustness and shape of the pelvic inlet, among other features (Arsuaga et al., 1999). The age of this individual, 350-500 kya (Bischoff et al., 2003), make it useful for understanding the transition in pelvic shape during the later stages of hominin evolution.

Material and methods

Modern primate material was measured at the Harvard Museum of Comparative Zoology in Cambridge, Massachusetts, the American Museum of Natural History in New York, New York, and at Kent State University in Kent, Ohio. In total, 58 Cercopithecines, 63 Hylobatids, 35 *Pan*, 30 *Gorilla*, 12 *Pongo*, and 38 *Homo sapiens* (Table 1).

Fossil cast material was measured from collections at the University of Michigan in Ann Arbor, Michigan. These included AL 288-1, Sts 14, and STW 431. KNM-ER 3228 (Rose, 1984) and SH1 (Bonmati et al., 2010) were examined from published photographs. BSN49/P27 measurements were taken on a cast provided by Scott Simpson at The Case Western Reserve in Cleveland, Ohio.

There is variation in the number of sacral vertebrae between species and to some extent within species. Furthermore, in large bodied primates, the last lumbar vertebra sometimes fuses with the first sacral vertebra and functionally becomes a part of the sacrum (Abitbol, 1987; Aiello and Dean, 1990). Due to a lack of functional difference between lumbar and sacral vertebrae under this circumstance, the sacrum was defined as the 3-7 vertebrae with fused spinous and transverse processes that articulate with the ilium (Abitbol, 1987).

Table 1. Primates Measured			
Species	Male	Female	Total
Hylobates lar lar	30	28	58
Hylobates klossi	1	1	2
Hylobates hoolock	-	3	3
Hylobates concolor	1	1	2
Pan troglodytes schweinfurthii	10	1	11
Pan troglodytes troglodytes	9	9	18
Pan troglodytes verus	3	3	6
Gorilla gorilla beringei	4	-	4
Gorilla gorilla gorilla	15	11	26
Pongo pygmaeus	5	7	12
Homo sapiens	17	21	38

This study refers to members of superfamily Hominoidea (hylobatids and hominids) as hominoids, members of family Hominidae (humans and large-bodied apes) as hominids, and members of tribe Hominini as hominins.

Surface Area Measurements

Surface area measurements were obtained from photographs that were taken using a Nikon camera and measured using the free software Image-J from NIH. Photos of the surfaces included in this study (SBA and ASA) were taken such that the plane of the camera lens was parallel to the articular surface.

Sacral body area (SBA) was measured by tracing the margin of the body (Figure 1); Image J then calculated the total number of pixels in the selected area and converted this to mm^2 using a calibration included in the frame of the photo.

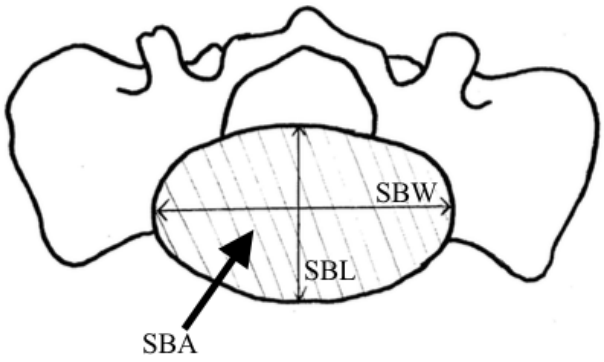

Figure 1. Showing measurements of the sacral body area (SBA) and linear sacral body dimensions, sacral body width (SBW) and sacral body length (SBL)

This measurement was obtained for all extant taxa and fossil specimens that preserved the sacrum (Sts 14, STW-431, AL-288-1, and BSN49/P27). Extant individuals that had a substantial amount of ostephytic growth around the margin of the sacral body were not included in this study.

Auricular surface area (ASA) was obtained by taking scaled photographs of auricular surfaces on the sacrum (Figure 2) except in the case of the fossil specimen KNM-ER 3228 where only the innominate was available; this measurement is shown in Figure 3. ASA was measured by tracing the margin of the surface, which Image J then converted to mm^2 using a calibration included in the photo. Generally, the auricular surface on the sacrum was measured instead of the ilium because it was more clearly discernable.

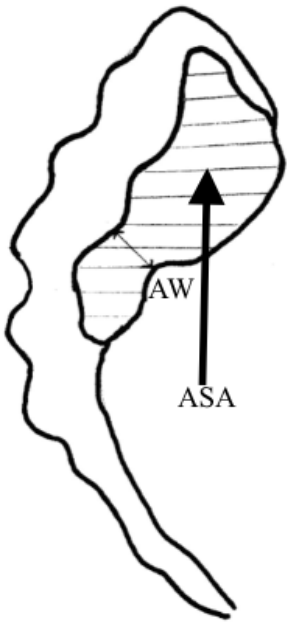

Figure 2. Showing measurements of the auricular surface area (ASA) on the sacrum and linear measurements of the surface, auricular width (AW)

Figure 3. Showing measurements of the auricular surface area (ASA) on the innominate

Linear Measurements

Linear measurements were made to the nearest 0.1mm using Mitutoyo Digimatic Calipers. In only two cases, fossil specimens KNM-ER 3228 and SH1, linear measurements were obtained from scaled photographs using ImageJ because physical casts were not available for measurement.

The acetabular diameter (AD) was assessed as the maximum craniocaudal diameter (Figure 4). As noted above, acetabular diameter was estimated from published photographs using ImageJ for KNM-ER 3228 (Rose, 1984) and SH1 (Bonmati et al., 2010). These measurements were compared with published dimensions for consistency (Ruff, 2010; McHenry, 1992).

Sacral width (SW) was defined as the maximum mediolateral width (Figure 5). Individual widths for each sacral element (S1-S5) were measured at the widest point on each element. These dimensions were taken on all extant individuals and one fossil specimen, AL-288-1, which preserved all sacral elements.

Sacral length (SL) was measured as the maximum cranio-caudal axial length measured from the ventral edge of the first and last sacral vertebrae (Figure 5). In cases where the sacrum was not fully fused, unfused elements were measured individually and summed for total length. SL was measured on all extant individuals and the fossil specimen AL-288-1, which preserves the sacral length.

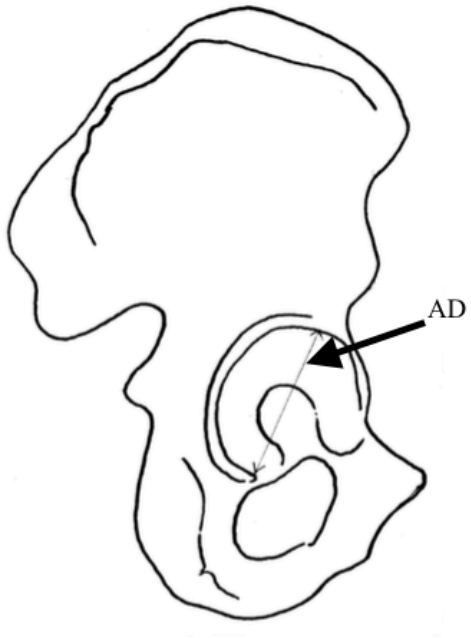

Figure 4. Showing measurements of the acetabular diameter (AD)

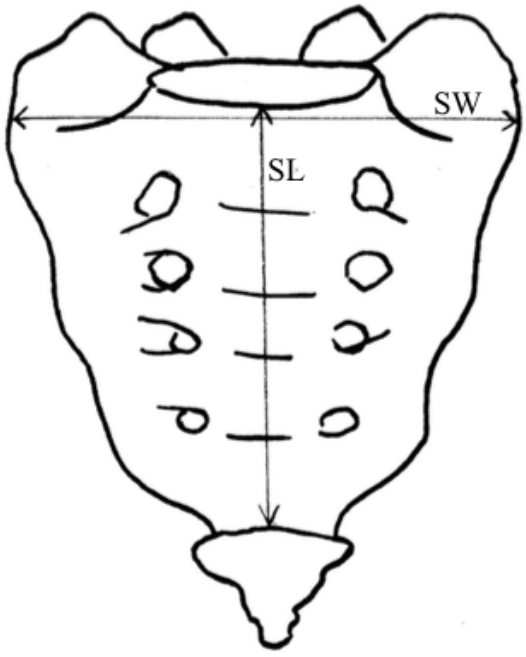

Figure 5. Showing measurements of the sacral length (SL) and sacral width (SW)

Data Analysis

Species included in this study were variable in size so joints included in this study (AD, ASA, and SBA) were $\log_{10}$ transformed to reduce the skew of the data and make taxa more comparable. Least squares linear regressions were used in body mass and joint scaling regressions using the SPSS statistics software. This included log transformed SBA, AD, and ASA individual regressed on log transformed body mass in addition to log transformed SBA and ASA regressed on log transformed AD. Body mass predictions were calculated from least squared regression line equations that included joints measured in this study and $\log_{10}$ transformed sex-specific species mean body masses obtained from published material (Smith and Jungers, 1997).

Statistical significance (<0.05) was determined using the Mann-Whitney U-test or Kruskal-Wallis test using Microsoft Excel statistical spreadsheets published on biostathandbook.com. Both intra- and interspecific tests comparing joint sizes as well as sacral element widths were performed this way.

Sacral tapering was examined by comparing percentages of each sacral width to overall sacral length. The variability in the number of sacral elements in sacrum was standardized by only including individuals from each taxon that had five sacral elements. S1-S5 measurements were each divided by total sacral length (SL) to get 5 different percentages for each individual measured.

Table 2. Measured Individuals by Sacral Length

	Number of Sacral Vertebral Elements *						
	1	2	3	4	5	6	7	Total
Cercopithecidae		10	45	3				58
Hylobates			3	30	24	7		64
Pongo				2	2	8		12
Gorilla				2	15	12	1	30
Pan					10	21	4	35
Homo Sapiens				3	30	3		36

*only includes individuals with complete sacrum available to record number of sacral vertebrae. Material preserving the articular surfaces was used even if the sacral elements were not entirely preserved.

Results

Almost all interspecific comparisons of raw joint data resulted in statistically significant (<0.05) differences. The exceptions to this were SBA and AD comparisons of both Human and *Gorilla* (SBA p= 0.58; AD p= 0.06) and *Pan* and *Pongo* (SBA p=0.5; AD p=0.84).

Species Means

Species means for acetabular diameter (AD), first sacral body area (SBA), and auricular surface area of the sacroiliac joint (ASA) for all primates measured are summarized in Table 3. Extant individuals that did not preserve all three pelvic joints were not included in these means, which in some cases (*Pan troglodytes troglodytes* and *Pongo pygmaeus*) substantially reduced the sample size.

Mann-Whitney U-tests only revealed significant intraspecific sex-based differences in three species. In *Gorilla*, all three joints were significantly different (p-

value<0.05) between males and females. *Pongo* has a significant intraspecific difference for AD measurements (p-value=0.01). *H. sapiens* also has a significant difference (p-value=0.002) in AD size between males and females.

Table 3. Summary of Species Means

Species	Sex	N	SBA	s.d. SBA	ASA	s.d. ASA	AD	s.d. AD
Macaca fascicularis	Male	11	146.618	29.91	117.856	22.93	15.247	1.12
	Female	10	100.916	9.66	79.542	12.43	13.008	0.53
Hylobates lar lar	Male	30	170.555	36.39	158.525	30.04	20.697	1.60
	Female	28	171.193	27.58	157.478	31.07	21.006	0.81
Pan troglodytes troglodytes	Male	9	700.357	96.85	612.261	73.96	41.559	2.81
	Female	9	644.587	104.36	581.055	109.94	39.328	1.25
Gorilla gorilla gorilla	Male	15	1409.632	203.70	1393.948	343.75	59.172	3.60
	Female	11	874.292	132.77	1009.402	175.69	47.955	2.45
Pongo pygmaeus	Male	5	787.984	143.00	918.895	404.76	46.116	2.58
	Female	7	623.664	193.47	538.478	117.39	38.579	1.66
Homo sapiens	Male	17	1278.822	254.21	1042.036	135.47	53.193	2.28
	Female	21	1193.265	193.31	1005.743	149.59	49.906	2.13
Australopithecus afarensis	AL-288 (F)	1	545.103		548.107		36.090	
Australopithecus africanus	STW-431 (M)	1	647.600		673.277		46.000	
	Sts 14 (F)	1	394.509		546.871		33.000	
Homo erectus	KNM-ER 3228 (M)	1			655.248		55.650	
	BSN49 (F)	1	655.36		789.61		41.000	
Homo heidelbergensis	SH1 (M)	1			1054.046		60.500	

Articular surfaces on body mass

Least squares linear regression coefficients for the regression of log_{10}-transformed mean joint size on log_{10}-transformed sex-specific means for body mass are shown in Table 4 and are separated into nonhuman hominoid and hominoid groups. Regressions for ASA on body mass are shown in Figures 6 and 7 for nonhuman hominoids and hominoids respectively. All regressions have high r^2 values indicating a close scaling relationship between joint size and body size. In all

Table 4. Least squares regressions of pelvic articular surfaces on body mass

Articulation	Taxa	r^2	Y-intercept	Slope
Auricular Surface (ASA)	Nonhuman	0.982	1.71	0.65
	Total	0.953	1.7	0.68
Acetabular Diameter	Nonhuman	0.993	1.09	0.31
	Total	0.954	1.08	0.32
First Sacral Body Area (SBA)	Nonhuman	0.990	1.77	0.62
	Total	0.916	1.75	0.66

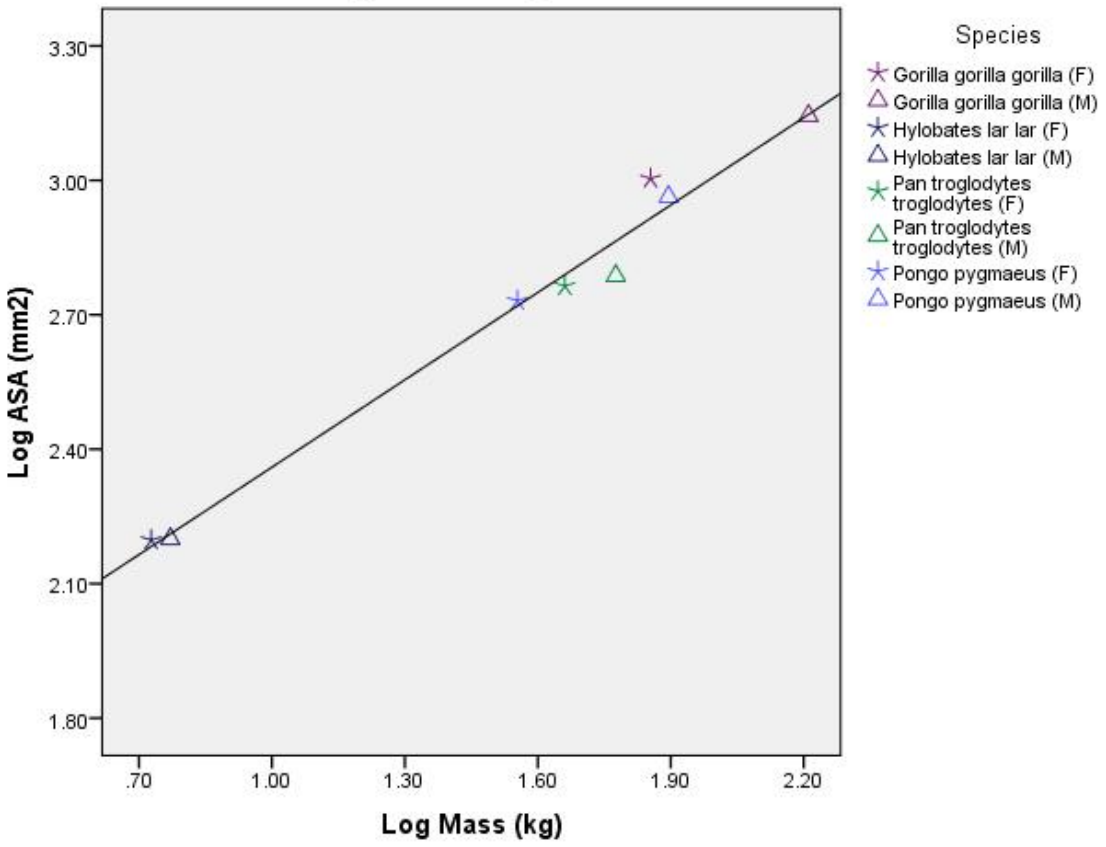

Figure 6. Regression of Log_{10} of ASA (mm^2) on log_{10} Mass (kg). Data points are sex-specific species means of nonhuman hominoids. In all cases male mean exceeds that of the female.

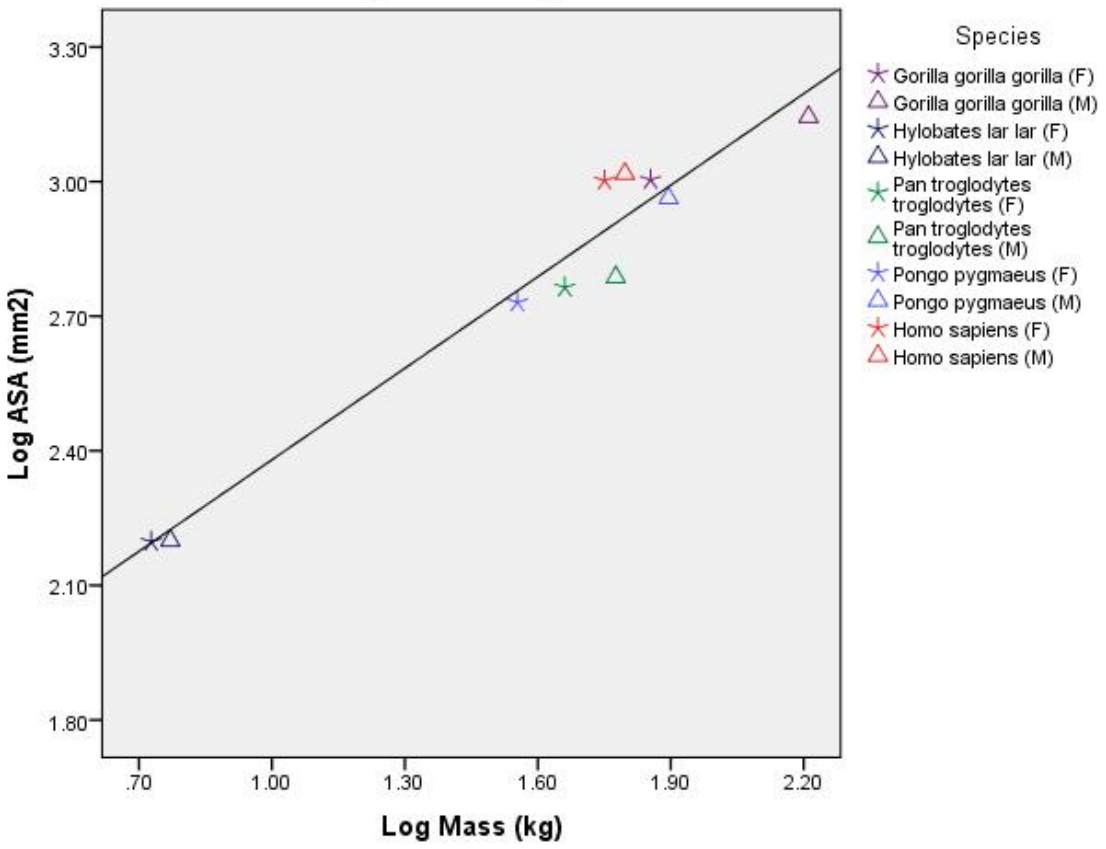

Figure 7. Regression of Log_{10} of ASA (mm^2) on log_{10} Mass (kg). Data points are sex-specific species means of hominoids. In all cases male mean exceeds that of the female

cases, the inclusion of humans into the samples lowers the r^2 value, suggesting a different scaling relationship for humans compared to other hominoids.

Least squares regressions for log AD on log mass are presented in Figures 8 and 9, both of which have high r^2 values. Least squares regressions for log SBA on log mass are presented in Figures 10 and 11, which both have high coefficients of correlation. In both cases, humans have relatively higher joint sizes than would be predicted for their body mass, compared to other hominoids.

Body mass predictions for 6 fossil hominoids represented by either sacra or ilia (STW-431, AL-288, BSN49/P27, Sts 14, KNM-ER 3228, and SH1) based on least squares regressions (Table 4) can be found in Table 5. SBA could not be used to predict body mass for the 2 fossils represented here only by an innominate (KNM-ER 3228 and SH1). The equations from Table 4 were used to estimate body mass in the fossil taxa. It is recognized the nonhuman hominoid sample is not ideal for estimating mass in bipeds (McHenry, 1992) however, it is deemed useful to compare these estimates to understand the relationship of pelvic joints to body mass.

Estimates based on nonhuman hominoid regressions resulted in higher body mass predictions for the fossil specimens represented here than estimates based on hominoids regressions. Regressions based on AD resulted in the highest body mass predictions except in the cases of the AL-288, BSN49/P27, and Sts 14 where ASA regressions produced the largest estimates.

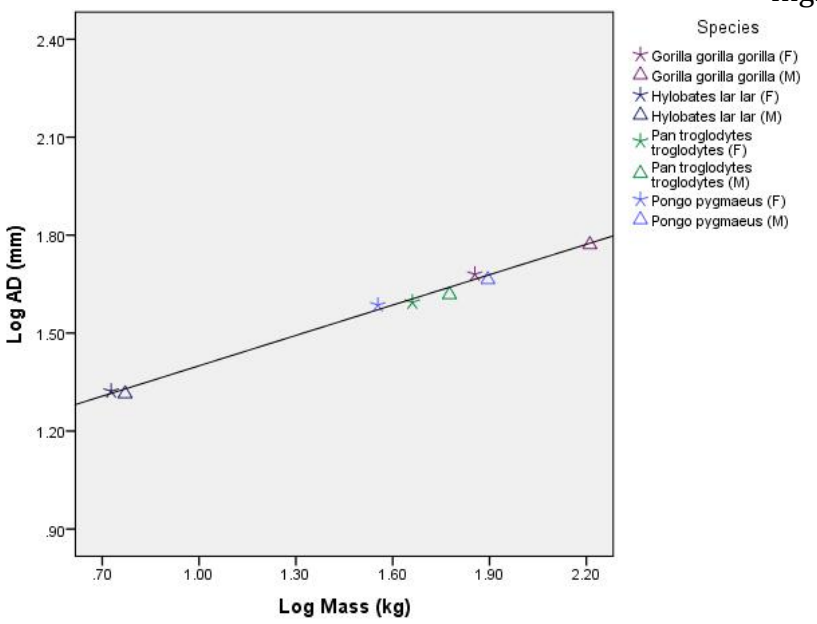

Figure 8. Regression of Log_{10} of AD (mm^2) on log_{10} Mass (kg). Data points are sex-specific species means of nonhuman hominoids. In all cases male mean exceeds that of the female.

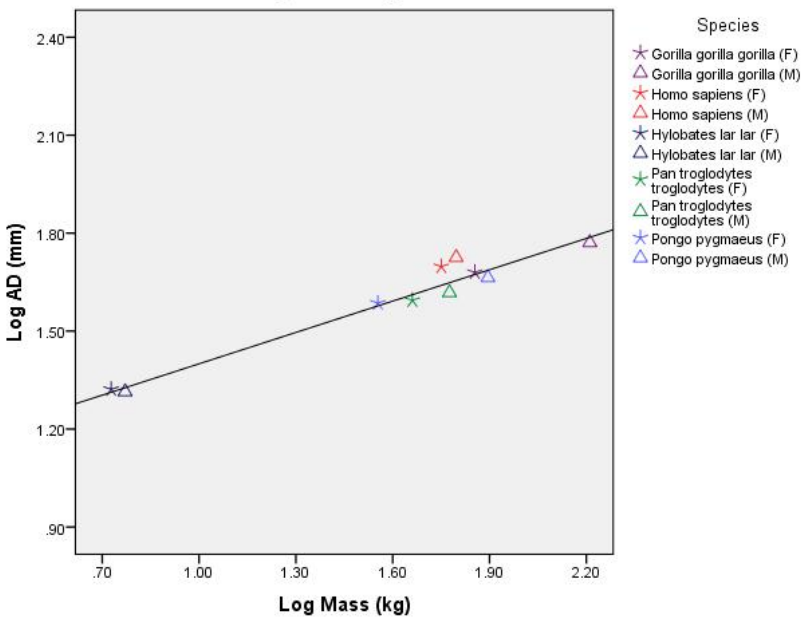

Figure 9. Regression of Log_{10} of AD (mm^2) on log_{10} Mass (kg). Data points are sex-specific species means of hominoids. In all cases male mean exceeds that of the female.

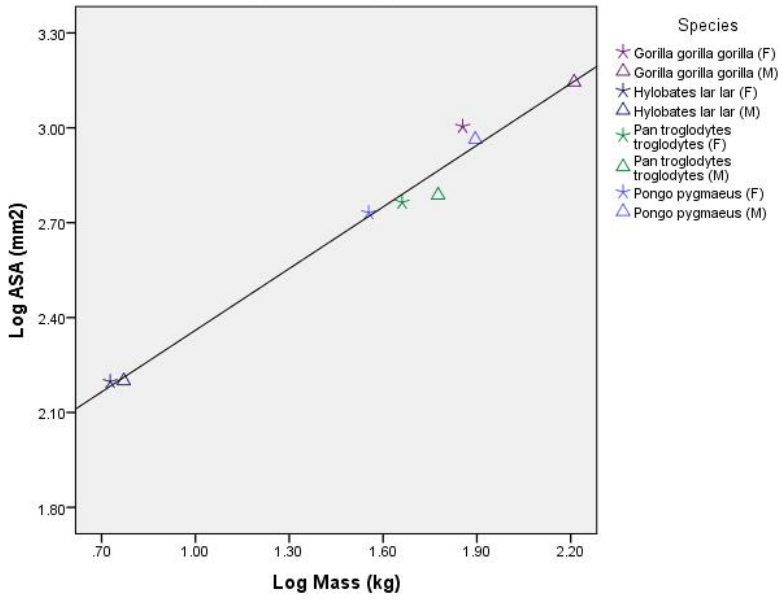

Figure 10. Regression of Log_{10} of SBA (mm^2) on log_{10} Mass (kg). Data points are sex-specific species means of nonhuman hominoids. In all cases male mean exceeds that of the female.

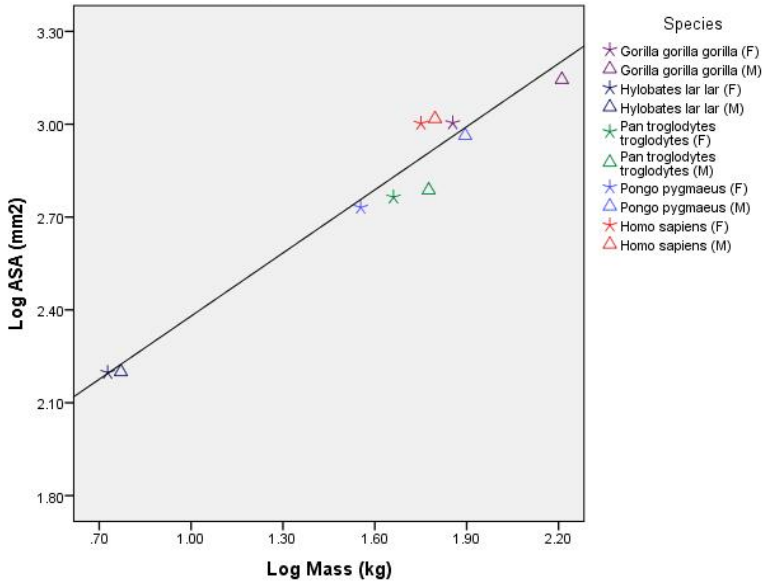

Figure 11. Regression of Log_{10} of SBA (mm^2) on log_{10} Mass (kg). Data points are sex-specific species means of hominoids. In all cases male mean exceeds that of the female.

Table 5. Body mass estimates based on articular surfaces				
	Group	ASA BME	SBA BME	AD BME
STW-431	Total	45.61	40.55	66.24
	Nonhuman	52.52	47.81	70.41
AL-288	Total	33.71	31.24	31.03
	Nonhuman	38.27	36.21	32.19
BSN49/P27	Total	57.58	41.28	46.23
	Nonhuman	67.01	48.72	48.57
Sts 14	Total	33.60	19.14	23.46
	Nonhuman	38.14	21.50	24.12
KNM-ER3228	Total	43.83	-	120.11
	Nonhuman	50.37	-	130.14
SH1	Total	88.18	-	155.95
	Nonhuman	104.66	-	170.40
Based on regressions in Table 5; BME (Body mass estimate); Kilograms				

Auricular surface area on acetabular diameter

Least squares regression statistics for the regression of log-transformed ASA on log-transformed AD are shown in Table 6 and plotted in Figure 12. The species mean regression of ASA on AD resulted in very high coefficients of correlation for both extant hominoid and extant nonhuman hominoid regression as did the regression of $\log_{10}$–transformed SBA on $\log_{10}$-transformed AD.

Intraspecific patterns of scaling were also examined. Figure 13 shows the *H. sapiens* regression with hominoid fossils for comparison. All fossil hominoids fall below the human regression line, and have small ASA for their AD size.

Within *Pan troglodytes troglodytes* there is a slightly higher coefficient of correlation between $\log_{10}$-transformed ASA and $\log_{10}$-transformed AD (r^2 =0.168). This relationship can be seen in Figure 14, which includes *P. t. troglodytes* and

Table 6. Pelvic joints regressed on acetabular diameter				
Regression	Group	r^2	y-int.	Slope
Auricular surface area (ASA) on Acetabular Diameter (AD)	All Hominoid (Species Means)	0.992	-0.58	2.1
	All Hominoid (Raw Data)	0.963	-0.55	2.09
	Nonhuman Hominoid (Species Means)	0.993	-0.61	2.12
	Nonhuman Hominoids (Raw Data)	0.959	-0.57	2.1
Sacral Vertebral Body Area (SBA) on Acetabular Diameter (AD)	All Hominoid (Species Means)	0.991	-0.51	2.07
	All Hominoid (Raw Data)	0.955	-0.51	2.08
	Nonhuman Hominoid (Species Means)	0.993	-0.42	2.01
	Nonhuman Hominoids (Raw Data)	0.957	-0.41	2.0

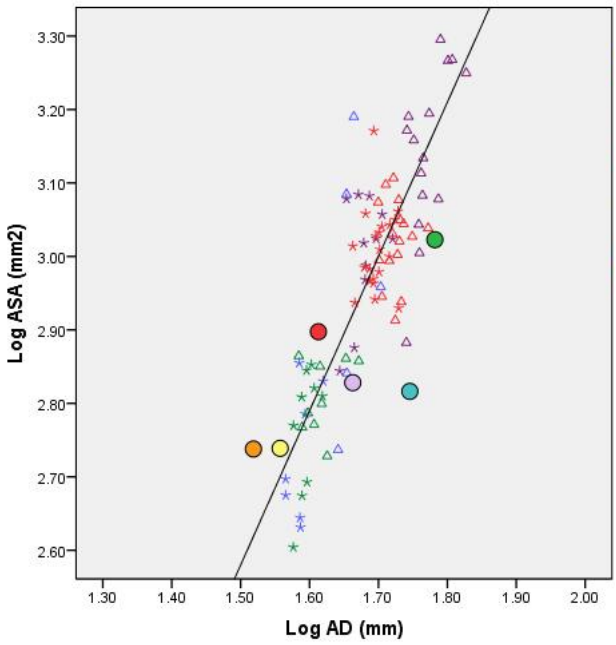

Figure 14. Regression of Log_{10} of ASA(mm^2) on log_{10} AD (mm^2). Data points are raw data from all hominoids. *Hylobates* are not shown but are included in the nonhuman hominoid least squares regression line. Species denoted by color (*Gorilla gorilla gorilla* = purple, *Homo sapiens* = red, *Pan troglodytes troglodtyes* = green, *Pongo pygmaeus* = blue, *Hylobates lar lar* = navy), Sex denoted by symbol (Male Δ, Female ⋆), Fossil individuals are filled in circles (AL-288=yellow, BSN49/P27 = red, KNM-ER 3228 = blue, SH1 = green, Sts 14 = orange, STW-431 = pink).

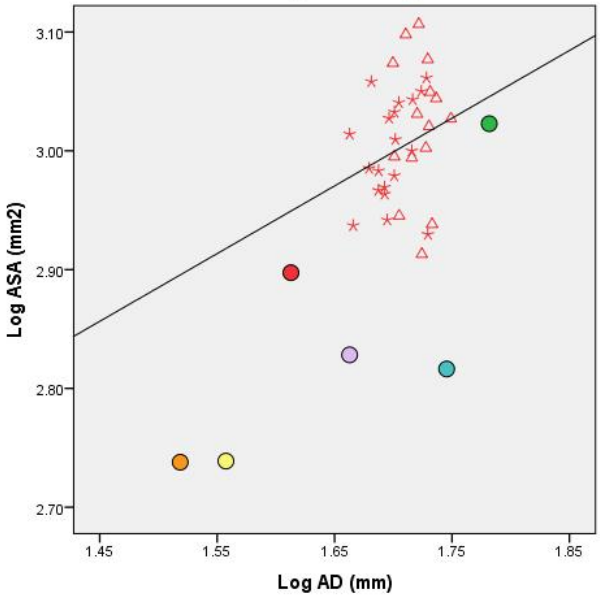

Figure 15. Regression of Log_{10} of ASA(mm^2) on log_{10} AD (mm^2). Data points are raw human measurements. $R^2 = 0.057$, y-intercept = 2.03, slope = 0.57; Data is labeled as in Fig.12

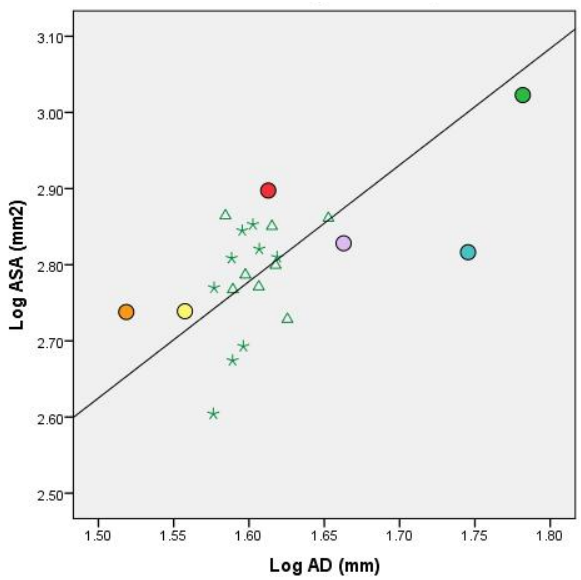

Figure 16. Regression of Log_{10} of ASA(mm^2) on log_{10} AD (mm^2). Data points are raw *Pan troglodytes troglodytes* measurements. $R^2 = 0.168$, y-intercept = 0.33, slope = 1.53; Data is labeled as in Fig.12

fossil hominoids for comparison. *Australopithecus* specimens and BSN49/P27, *H. erectus*, fall within the variation of *Pan*.

Gorilla gorilla gorilla has a moderately high coefficient of correlation for the least squares regression of $\log_{10}$-transformed ASA and $\log_{10}$-transformed AD (r^2 =0.526; Figure 15). The fossil hominins included fall at the low end of the *G. g. gorilla* data spread with SH1 falling comfortably within the data and Sts 14 being most distant from the majority of the *Gorilla* data. SH1, KNM-ER 3228, and STW-431 all exhibit AD measures that fall within the range of *Gorilla.*

Pongo pygmaeus has a coefficient of correlation for $\log_{10}$-transformed ASA and $\log_{10}$-transformed AD of r^2 =0.572. This relationship can be seen in Figure 16 where fossil hominoids are included for comparison.

Sacral body area on acetabular diameter

Regressions of the SBA on AD for all groups discussed below are listed in Table 6. The coefficient of correlation between these joints is high in both hominoids and nonhuman hominoids (r^2 =0.99). This relationship plotted with fossil hominins can be seen in Figure 17.

All fossil hominins represented here either fall within the scatter of extant hominoids except Sts-14, which has an absolutely small SBA and AD. Therefore this likely represents an individual smaller than any of the hominids in this study.

Intraspecific patterns of scaling were also examined. The regression of $\log_{10}$–transformed SBA on $\log_{10}$–transformed AD for humans is shown in Figure 18. The

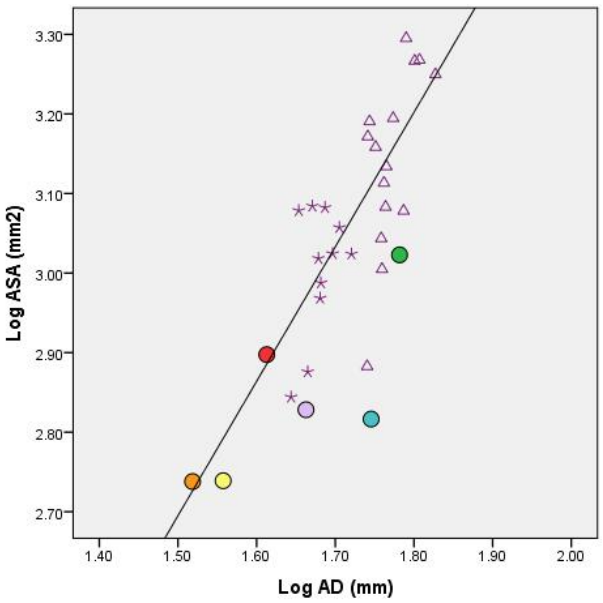

Figure 15. Regression of Log_{10} of ASA(mm^2) on log_{10} AD (mm^2). Data points are raw *Gorilla gorilla gorilla* measurements. $R^2 = 0.526$, y-intercept = 0.16, slope = 1.69; Data is labeled as in Fig.12

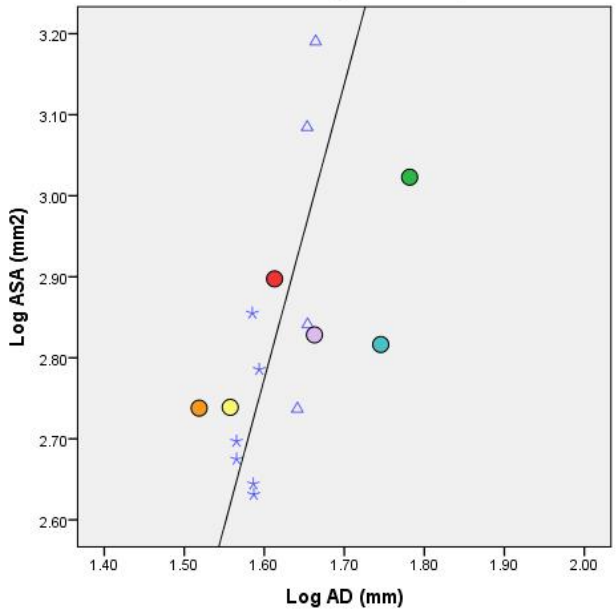

Figure 16. Regression of Log_{10} of ASA(mm^2) on log_{10} AD (mm^2). Data points are raw *Pongo pygmaeus* measurements. $R^2 = 0.572$, y-intercept = -3.05, slope = 3.64; Data is labeled as in Fig.12

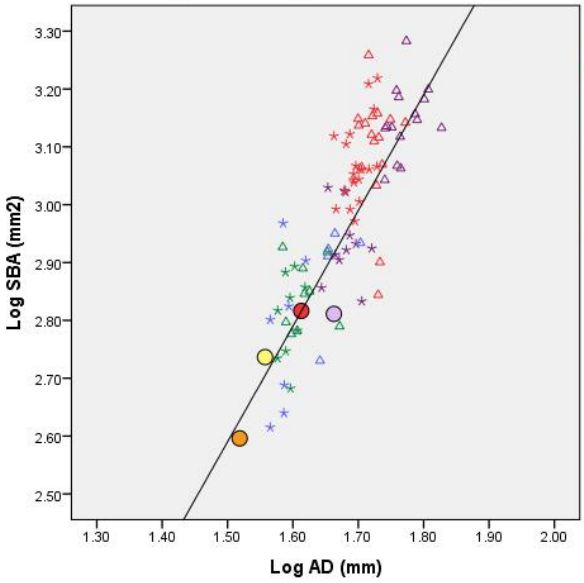

Figure 17. Regression of Log_{10} of SBA (mm^2) on log_{10} AD (mm^2). Data points are raw data from all hominoids. *Hylobates* are not shown but are included in the nonhuman hominoid least squares regression line. Data is labeled as in Fig.12

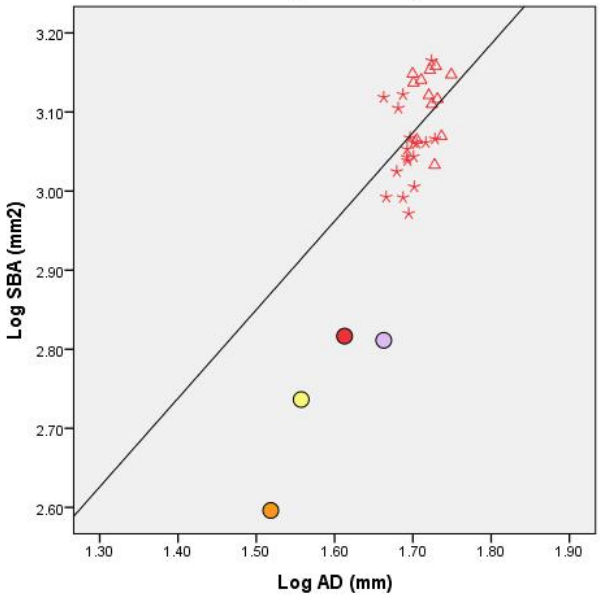

Figure 18. Regression of Log_{10} of SBA (mm^2) on log_{10} AD (mm^2). Data points are raw *Homo sapiens* measurements. R^2 = 0.18, y-intercept = 1.17, slope = 1.12; Data labeled as in Fig. 12

fossil hominins all exhibit both a smaller AD and smaller SBA than any extant human sampled.

The *P. t. troglodytes* least squares regression between the SBA and the AD is show in Figure 19 with fossil hominoids plotted for comparison. AL-288-1, BSN49/P27, and STW-431 have SBA measurements that fall within the spread of the *Pan* data. STW-431 has a slightly higher AD than observed in any *Pan* individuals represented here. Sts 14 falls below the least squares regression in Figure 19 indicating both a smaller SBA and smaller AD than any *P. t. troglodytes* measured in this study.

The $\log_{10}$-transformed SBA plotted against $\log_{10}$-transformed AD for *G. g. gorilla* (r^2 =0.651) is plotted in Figure 20 with fossil hominoids added in for comparison. There is no overlap in male and female *G. g. gorilla* data with males having both relatively larger SBA and AD measurements than females. The fossil specimens, while smaller in size, fall fairly close to the gorilla regression line, suggesting similar scaling patterns.

In *Pongo pygmaeus*, the least squares regression of $\log_{10}$-transformed SBA on $\log_{10}$-transformed AD is shown in Figure 21. The fossils represented here fall close to the regression line. Overall, the fossil taxa have SBA joints that are smaller than those of humans but within the range of *Pongo* and *Pan*. The scaling relationship most closely resembles that of *Gorilla*.

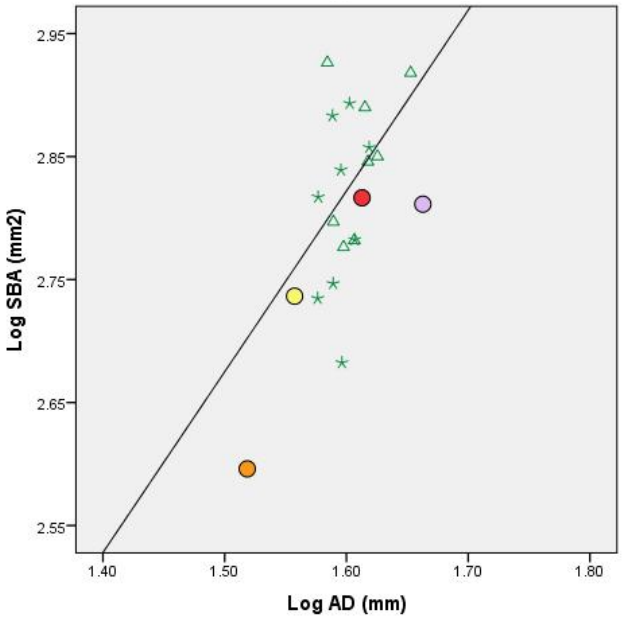

Figure 19. Regression of Log_{10} of SBA (mm^2) on log_{10} AD (mm^2). Data points are raw *Pan troglodytes troglodytes* measurements. $R^2 = 0.175$, y-intercept = 0.47, slope = 1.47; Data labeled as in Fig. 12

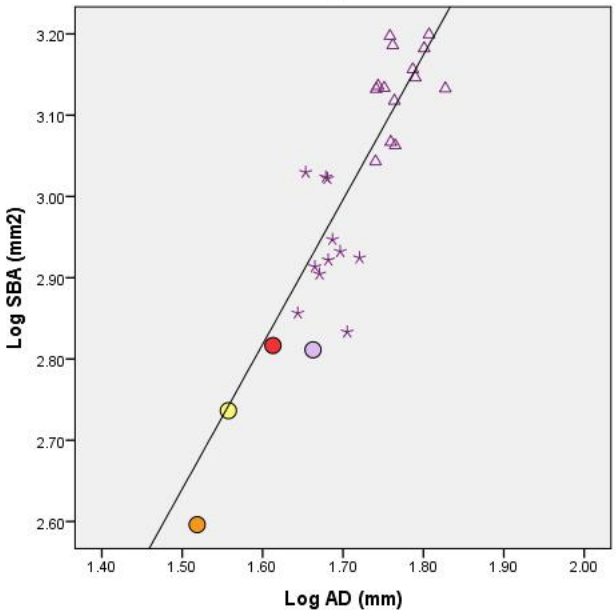

Figure 20. Regression of Log_{10} of SBA (mm^2) on log_{10} AD (mm^2). Data points are raw *Gorilla gorilla gorilla* measurements. $R^2 = 0.651$, y-intercept = -0.03, slope = 1.78; Data labeled as in Fig. 12

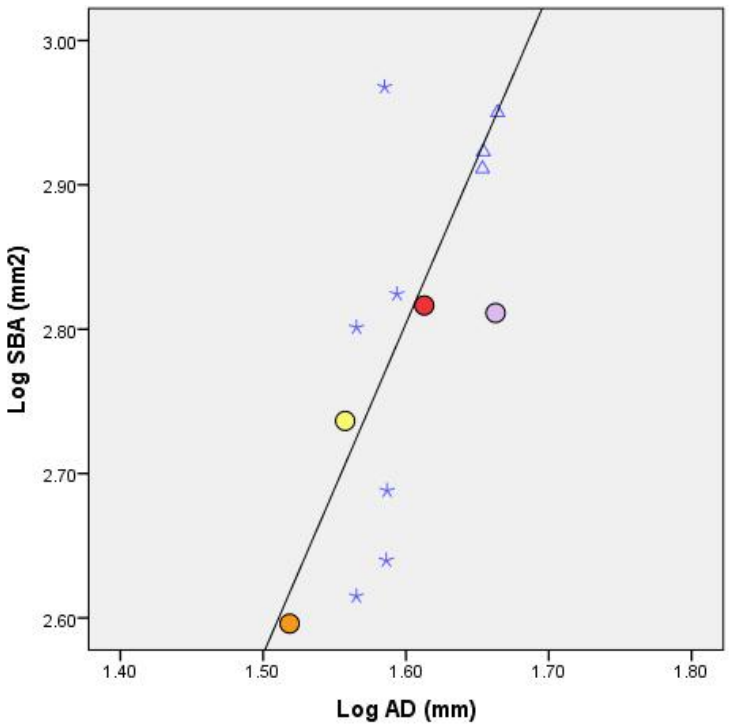

Figure 21. Regression of Log_{10} of SBA (mm^2) on log_{10} AD (mm^2). Data points are raw *Pongo pygmaeus* measurements. $R^2 = 0.443$, y-intercept = -0.86, slope = 2.29; Data labeled as in Fig. 12

Sacral tapering

The ratios of the width of individual sacral elements (S1-S5) divided by total sacral length (SL) are provided in Table 7. Included in this comparison is fossil individual AL-288-1, *Australopithecus afarensis*, the only fossil specimen for which there is a complete sacrum. These percentages are plotted in Figure 22 to show the change in overall sacral shape.

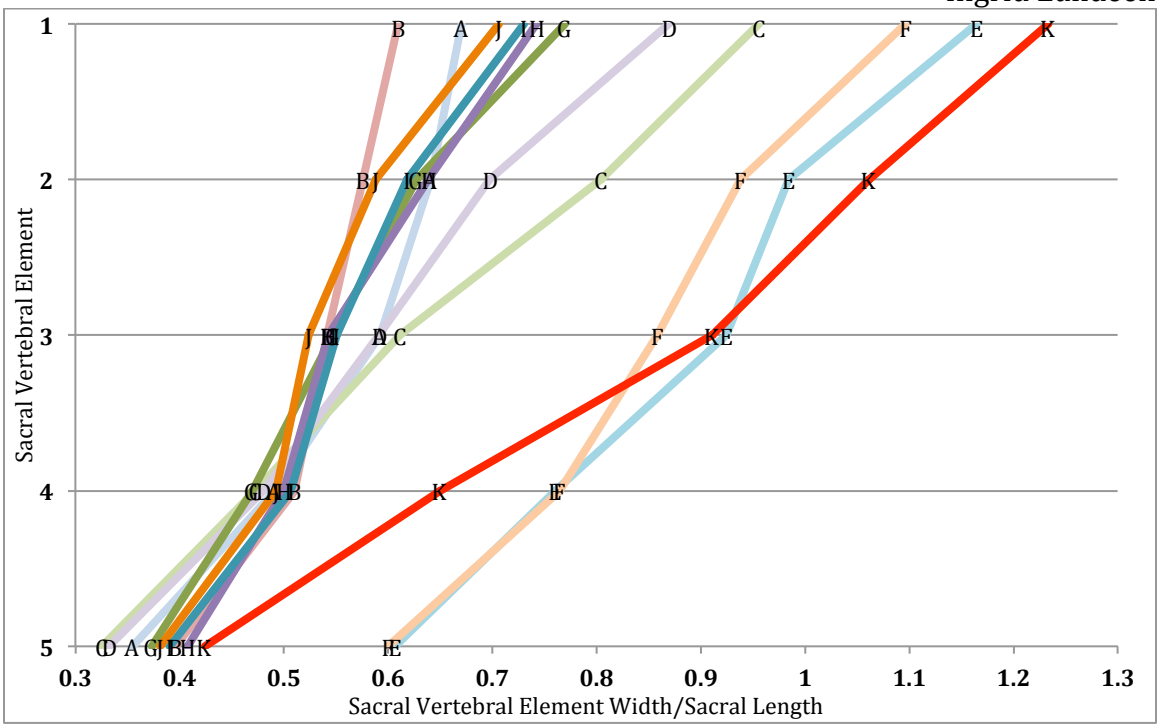

Figure 22. Interspecific comparison of sacral vertebral elements/sacral length. A= *Gorilla gorilla gorilla* (Female); B = *Gorilla gorilla gorilla* (Male); C = *Hylobates lar lar* (Female); D = *Hylobates lar lar* (Male); E = *Homo sapiens* (Female); F = *Homo sapiens* (Male); G = *Pongo pygmaeus* (Female); H = *Pongo pygmaeus* (Male); I = *Pan troglodytes troglodytes* (Female); J = *Pan troglodytes troglodytes* (Male); K =AL-288, *Australopithecus afarensis* (Female)

Table 7. Sacral Element Ratios

		Sacral Vertebral Element/ Total Sacral Length					Shape Change
	Sex	1	2	3	4	5	S1-S5
G.g.gorilla	F	0.6708	0.6407	0.5925	0.4912	0.3548	0.315
G.g. gorilla	M	0.6099	0.5759	0.5416	0.5103	0.3958	0.214
H.l. lar	F	0.9558	0.8041	0.6114	0.4725	0.3254	0.630
H.l. lar	M	0.8693	0.6974	0.5913	0.4802	0.3319	0.537
H. sapiens	F	1.1646	0.9844	0.9244	0.7600	0.6068	0.557
H. sapiens	M	1.0963	0.9378	0.8580	0.7643	0.5997	0.496
P. pygmaeus	F	0.7698	0.6273	0.5472	0.4697	0.3735	0.396
P. pygmaeus	M	0.7423	0.6388	0.5430	0.4997	0.4075	0.334
P.t. troglodytes	F	0.7303	0.6184	0.5506	0.5068	0.3905	0.339
P.t. troglodytes	M	0.7064	0.5883	0.5239	0.4927	0.3814	0.324
Australopithecus afarensis (AL-288)	F	1.2334	1.0613	0.9111	0.6497	0.4241	0.809

While all extant taxa exhibit tapering from S1-S5, this decrease is most dramatic in *Homo*, where sacral width decreases from 100% to 60% of the sacral length. The other taxa have a narrower sacrum in all elements, S1-S5, and taper from 40%-60% to 35% of the sacral length. AL-288-1 has a unique pattern, with a relative breadth at S1 matching that of *Homo* (~100% of the length), but with a relative breadth at S5 similar to those of nonhuman hominoids (~40%).

Intraspecific comparisons were carried out using Mann-Whitney U-tests. Only three species had a significant difference between male and female element percentages. Humans had significantly different S1 (p-value=0.002), S2 (p-value=0.003), and S3 (p-value=0.002) percentages. *Gorilla* has different S1 (p-value=0.026), S2 (p-value=0.007), and S5 (p-value=0.01) percentages. *Hylobates* had significantly different S1 (p-value=0.02) and S2 (p-value=0.016) percentages.

Kruskal-Wallis tests revealed significant interspecific differences in each sacral element (p-values<0.05). Among caudal elements (S3-S5) of hominids, Mann-Whitney U-tests revealed significant differences between humans and each of the nonhuman hominids but no significant relationship between nonhuman hominid species. In addition, when hominoids were compared, *Hylobates* was significantly different from *Pan* for S3 (p-value=0.003) and S5 (p-value=0.002) percentages. The S5 percentages for *Hylobates* were significantly different from *Pongo* (p-value=0.03)

Discussion

Articular surfaces on body mass

There is considerable interest in reconstructing body mass in fossil hominoids as mass is tied to several critical aspects on an organism's biology, including its locomotion, diet, life history and reproduction (Ruff, 1991). Previous studies have shown that body mass predictions are reliably calculated using postcranial joint areas and linear dimensions because these joints have a more direct relationship to body size than other elements (Jungers, 1988, 1991; Ruff et al., 1989; Auerbach and Ruff, 2004). Articular surface dimensions also tend to be less influenced by changes in muscular loading or activity level during an individual's lifetime than cross sectional properties (Ruff, 1988; Lieberman et al., 2001; Auerbach and Ruff, 2004).

In this study, least squares regressions of sacral and pelvic linear dimensions and areas on body mass estimates from the literature (Smith and Jungers, 1997) among extant hominoids revealed a strong linear relationships (r^2 values ranged between 0.92 and 0.99). However, humans consistently had slightly larger sacral and pelvic joint sizes for their body mass than other hominoids, with the exception of male *Gorilla*. Previous studies examining hindlimb joint scaling relationships have reported similar results which has been attributed to larger loads, on average, being applied to hindlimbs in bipeds when compared with more quadrupedal primates (Jungers, 1988, 1991; Ruff, 1988; Ruff et al., 1989).

Of the three joints regressed on body mass, acetabular diameter had the highest coefficient of correlation for both hominoid and nonhuman hominoid groups, although all three had very high R^2 values. The ASA likely had the lowest coefficient of correlation because the joint varies in size and shape through adulthood (Bowen and Cassidy, 1981; Vleeming et al., 1990). In fact, the actual placement of the joint can change considerably during the lifetime of a human (Bowen and Cassidy, 1981). The interlocking structure at this joint has been hypothesized to more effectively transmit force through the joint by increasing articulating surface areas (Vleeming et al., 2007). However, the nature of this joint has not been fully explored in nonhuman primates so it is not clear if the surface morphology plays a role in the stability of the joint during bipedality or is simply a result of greater loading due to increased body mass. Despite this variation, this joint is worthy of study because there is no siginificant movement at the joint and therefore it is not affected by selection for range of motion, which some propose as having an effect on joint size (Swartz, 1989). Furthermore, this joint is subjected to massive load transmitting forces and has a strong relationship with body mass.

Compared with predictions calculated in previous studies from modern human samples (Ruff et al., 1997; Auerbach and Ruff, 2004; Ruff, 2010), body mass calculations in this study (Table 5) were calculated from regressions dominated by nonhuman primates. These nonhuman primates have relatively small hindlimb joints for their body size compared to bipeds, and so the body weight estimates from this study are uniformly higher than previous studies. Furthermore, this study

used mean sex-specific body mass of each species from the literature, as has been used in studies such as McHenry (1992); however, Ruff and colleagues (1991) use individual body mass. Thus, the body mass estimates presented here unlikely to be accurate, but will be discussed below as a tool for understanding the relationship between joint size and body mass.

As noted in other studies, AD had a strong relationship with body size. In some individuals, KNM-ER 3228 and SH1, remarkably large body masses were calculated. This can be attributed to the inclusion of male *Gorilla* in this regression. Both fossils had absolute AD measurements that fell at the upper end of the human range but well within *Gorilla* absolute sizes. A human-only regression with individual body masses would more accurately calculate body weight in these later *Homo* specimens.

In general, ASA produced the highest body mass predictions for all fossil individuals. BSN49/P27 had an ASA estimated body mass that was significantly higher than previously recognized by Ruff (2010). The predictions attained in this study, ASA predicted 57.58 kg and AD predicted 46.23 kg, contrast sharply with Ruff's estimate, based on femoral head dimensions, of 33.2 kg. Although the estimates presented here have already been acknowledged to be too high, the substantial difference between ASA and AD predicted body masses suggests that if a more comparable sample, i.e. modern *Homo* with associated body masses, was used, higher estimates for body mass based on ASA would be calculated for this fossil

individual. This larger body mass estimate would be relevant in discussion of this individual's taxonomic assignment.

Ruff (2010) argues against BSN49/P27 being *Homo erectus* because the estimated body mass of this specimen is startlingly small for a *H. erectus* individual, the smallest of which is KNM-ER 1472 with a body mass of 41.7kg. If a larger body mass estimate were calculated, as one based on ASA would likely present, it would be more reasonable to consider this individual *H. erectus*. However, the intermediate age of BSN49/P27 (0.9-1.4 Ma; Simpson et al., 2008) suggests that the body mass of this individual might not be relevant to its taxonomic assignment as individuals from this time period can be variable in size (Simpson et al., 2013).

For most of the fossil specimens, SBA produced the smallest body mass estimations. The exception to this was AL 288-1 where AD produced the smallest prediction (Table 5). The large body mass predictions from the ASA and the small body mass predictions from the SBA may be due to higher average forces being transmitting through the auricular surface than the sacral body area (Pal, 1989). A study done by Pal and Routal (1987) explained this phenomenon where the sacral angulation at the lumbo-sacral junction forces the L5 to slip slightly anteriorly, reducing stress directly onto the S1 body and increasing reliance on the zygopophyseal articulation and iliolumbar ligament. The stronger of the two components of the iliolumbar ligament, the lumbosacral ligament, transfers some of the load from the lumbar vertebrae directly to the alae of the first sacral element, essentially bypassing the L5-S1 articulation (Pal, 1989). This force is then

transmitted through the auricular surface and is noted to be 12% larger than the force transmitted through the L5-S1 articulation (Pal, 1989). This may account for the relatively higher body mass predictions for the auricular surface area in this study.

Joint Scaling

The scaling relationship between joints in fossil hominins may reveal whether that individual loaded its hindlimbs more like extant bipeds or climbing quadrupeds. In fossil genera, such as *Australopithecus,* there are debates over whether the species within this genus exhibited habitual bipedal (e.g. Lovejoy, 1978, 1988) or a combination of bipedal and arboreal actions (e.g. Stern and Susman, 1983). McHenry (1991) compared AL-288-1 to an Akka Pygmy individual, a modern human, and found that despite comparable body size, the sacral body dimensions were larger in the modern human which suggests that AL-288-1 was not loading this joint in the same way as modern humans. One way to further examine this debate is to determine whether the sacral body, sacroiliac and acetabular joint surfaces scale to one another in a way more similar to that of bipeds or quadrupeds. The results of this project reveal joint surface scaling relationships for the small bodied fossil hominins (AL-288-1, Sts 14, STW 431, and BSN49/P27) that tend to resemble patterns found in *Pan troglodytes troglodytes* rather than in *Homo sapiens*, perhaps indicating a force distribution pattern closer to what we see in modern chimpanzees than in modern humans (Figures 14,15,19, and 20).

As has been reported in previous studies, humans have relatively larger hindlimb joint sizes than non-bipeds due to these joints being subject to higher loading (Jungers, 1988, 1991). Significant intraspecific variation in ASA was seen within *G. g. gorilla* (p-value= 0.002), a species with high body size dimorphism. This would imply that ASA is very directly tied to body mass increases. Given this assumption, it would be fair to expect that there would be significantly different ASA measures for intraspecific comparisons in other highly dimorphic primates, such as *Pongo*. However, a Mann-Whitney U-test revealed no significant difference between male and female *Pongo* individuals (p-value= 0.08) which implies that there may be other factors that influence the ASA besides body mass. Jungers (1988) found that when only male hominoids were compared, *Pongo* had relatively smaller hindlimb joints than would be expected given their body size. Evidently, body size is not the only factor that bears on joint size in this species. In the case of *Pongo*, for example, their highly arboreal and suspensory positional behavior may ameliorate the effects of body size and reduce the loading experienced at joints.

An examination of the scaling of ASA on AD (Figures 13), all indicated *Australopithecus* specimens included in this study (AL 288-1, Sts 14, and STW 431) and female *Homo erectus*, BSN49/P27, fall within and around the range of variation exhibited in modern *P. t. troglodytes*. Purported female fossil individuals (AL 288-1, Sts 14, and BSN49/P27) tend to fall above the least squares regression line, indicating a larger ASA than would be expected for the given AD. While no statistically significant difference in AD was noted between males and females in

Pan, there was a significant difference between males and females in humans, *Gorilla,* and *Pongo*. The position of the purported male and female fossils might indicate a significant difference in AD between sexes in hominins.

BSN49/P27, a female *Homo erectus* was given this taxonomic assignment on the basis of traits such as an anteroposteriorly broadened birth canal, thickened acetabulocristal buttress, a shelf formed by attachment of the reflected head of the rectus femoris muscle, deepened fossa for the gluteus medius muscle, and expanded retroauricular area all of which are derived characters that are shared with *Homo* (Simpson et al., 2008). However this individual also shares plesiomorphic characters with early Pleistocene hominins including laterally flaring ilia, wide greater sciatic notches, small auricular surfaces, and anteriorly placed iliac pillars (Simpson et al., 2008, 2014). Due to the presence of these primitive characters and the small body size of this individual, it has been suggested that it may represent *Paranthropus boisei* (Ruff, 2010).

This study highlights the difficulty in assigning BSN49/P27 to a taxon. This individual exhibits much larger ASA and SBA than any small-bodied fossils included here (AL 288-1, Sts 14, and STW 431) and instead is more similar in size to members of genus *Homo* (Figure 13 and 18). Berge and Kazmierczak (1986) have noted that a small ASA is a key primitive hominin condition and is retained in some *H. erectus* individuals, such as KNM-ER 3228 (Rose, 1984), however BSN49/P27 has a relatively large ASA. Joint size may not be as useful as other features in determining taxonomic identity for these intermediate specimens. Recent discovery

of a *Homo erectus,* KNM-ER 5881b (Ward et al., 2015), which has a femoral head diameter that falls well within the range of australopiths, supports the idea that absolute joint size may not be useful for differentiating between late *Australopithecus* and *Homo*.

Regardless of taxonomic assignment of these individuals, the relationship between the joints seen in the fossil hominins included here is quite different than we see in modern humans, particularly for the early *Homo* individuals (KNM-ER 3228 and SH1) which both have much smaller ASA measurements than would be predicted from their AD. This may be a consequence of potential dimorphism (discussed above), as both fossil individuals have been identified as male, or it could be an indication that these early hominins exhibited a different pattern of loading than we see in modern *Homo*. Interestingly, KNM-ER 3228 is noted to have the derived condition of an expanded retroauricular surface area for increased ligamentous reinforcement around the SIJ (Rose, 1984). This suggests that reinforcement around the joint was important in force dissipation and likely preceded the increase in ASA size. A study done by Pal (1989) postulated that heavy ligamentous reinforcement of the SBA may allow for a smaller surface area at this joint. It seems reasonable to assume a similar condition may be present in hominins that exhibited small auricular surface areas but large ligament attachment sites, an idea that deserves further investigation.

While most of the fossil hominin joint sizes measured here fall within the range of variation found in *Pan*, SH1, reported to be *Homo heidelbergensis*, falls

within the range of variation found in both *H. sapiens* and *G. g. gorilla.* This is a reflection of the large absolute size of the acetabulum but does not necessarily reflect a similarity in loading pattern to *Gorilla*. As the most recent fossil included in this study (0.5 Ma) this increase in size and similarity in joint scaling relationship seems to represent a member of a group of hominins that had similar hindlimb loading patterns to those seen in modern humans when compared with earlier hominins, such as *Australopithecus africanus*. This supports the theory that a major increase in hindlimb joint size occurred late in hominin evolution and accompanied increased loading in hindlimbs, similar to that which we see in modern humans (McHenry, 1986; Jungers, 1988).

Sacral Tapering

An increase in sacral width relative to the first sacral body is noted in *Australopithecus* and is often discussed in the context of decreasing the distance between the SIJ and the acetabulum (Robinson, 1972; Stern and Susman, 1983; Lovejoy, 1988; Aiello and Dean, 1990; Sanders, 1995). It is hypothesized that the increase in width of the sacrum occurred in conjunction with a reduction in the height of the ilia, which together would have decreased the distance between the SIJ and AD, reducing stresses on the ilia when the full weight of the upper body was applied to them (Aiello and Dean, 1990). Additional obstetric benefits to increasing the overall true pelvis size to accommodate larger brained infants have also been proposed to explain sacral widening in *Australopithecus* (Robinson, 1972;

Leutenegger, 1972, 1974, 1977; Tague and Lovejoy, 1986; Aiello and Dean, 1990). The possibility that this increase in width is linked to sexual dimorphism within fossil forms has also been proposed but not well supported due to the lack of fossil sacral material (Robinson, 1972; Leutenegger, 1974). This study showed that females have relatively wider first sacral elements than males of the same species (Figure 6; Cheng and Song, 2003). There were statistically significant differences between the males and females in the cranial sacral elements in *Hylobates* (S1 and S2), *Gorilla* (S1, S2, and S5), and humans (S1-S3). Except in the case of *Gorilla* where a significant difference between males and females was also noted in the S5 (p-value = 0.01), any species that exhibited significant differences in sacral widths did so in the cranial sacral elements. As these are the elements that articulate with the ilia and form part of the bony pelvic ring it would be fair to assume that they would be most related to obstetric benefits of increasing sacral element widths. The significant differences shown in this study are consistent with this assumption.

Humans have wider sacral elements relative to the total sacral length when compared with *Gorilla* (p-value= 0.01), *Pan* (p-value= 0.01), and *Pongo* (p-value= 0.03), shown in Figure 6. This is not unexpected given the mechanical and obstetric reasons behind increase in true pelvis size. AL-288-1 also has a relatively wide S1, agreeing with earlier studies that have noted a broad pelvic inlet and a short and broad sacrum in *A. afarensis* (Berge and Kazmierczak, 1986; Tague and Lovejoy, 1986; Ruff, 1991).

One clear shape difference among hominoids in sacral tapering is the difference between the caudal elements of humans versus nonhumans (Figure 22). The human distal sacral elements remain relatively wide while *Pan, Gorilla, Pongo,* and *Hylobates* sacra taper more dramatically (Figure 22). Humans, both male and female, have fifth sacral elements (S5) that are still 60% of the overall length of the sacrum. In contrast, *Pan, Gorilla, Pongo,* and *Hylobates* all have S5s that are between 40% and 30% of the total length. The variation observed in the sacral tapering in different species of hominoid might stem from either load bearing or muscular attachments on the caudal portion of the sacrum.

Mahato (2010) has suggested that sacral shape is a result of the weight-bearing nature of these bones that causes "stockpiling" of the vertebral segments and the compression into a "compact triangular bone." This increase in force applied to the bones causes sacral elements of humans to be relatively wider than other hominoids and fuse more frequently in bipedal species (Mahato, 2010; Filler, 1994). This more frequent fusion of the bones in humans allows stability at the expense of mobility (Mahato, 2010).

An alternative explanation for the lack of sacral tapering in humans relates to the mechanical advantage afforded to piriformis muscle. The piriformis muscle is a lateral rotator of the thigh that arises from the ventral surface of the lower sacral elements and inserts on the highest point of the greater trochanter, playing an important role in pelvic stabilization during the single support phase of bipedal progression (Aiello and Dean, 1990). In biomechanical studies of human pelvic

muscles that examined anterior-posterior, superior-inferior, and medial-lateral planes, the piriformis muscle had the second highest muscular contribution to medial-lateral motion (Correa et al., 2010). Humans, compared with other extant apes, have a much shorter lever arm for the piriformis. This would bring the origin of the muscle closer to the point of rotation at the acetabulum and allow faster action of this muscle, as would be necessary in maintaining stability when walking upright. In contrast, species without wide lower sacral elements would have a much longer lever arm giving them more muscular strength but slower action.

The auricular surface of the sacroiliac joint is vertically oriented and is thus vulnerable to gravitational forces acting on body mass to displace the ilial and sacral surfaces of the SIJ in bipedal stances. Most studies have described the ligaments that surround the SIJ as being strong enough to withstand this vertical force (Grieve, 1983; Vleeming et al., 1990). However, some have proposed that as a transversely oriented muscle, the piriformis can produce SIJ compression and thus brace both the sacroiliac and hip joints in this upright posture (Snijders et al., 1998). A study by Snijders et al. (1998) found that transversely oriented muscles of the pelvis play a substantial role in helping to stabilize the SIJ through lateral compression (1998). Another study put forth the idea that the piriformis muscle may be important in locomotion by applying compressive forces to the proximal femur and preventing stress fractures when vertical force is applied to the femoral neck, (Michaud, 2012). Both of these studies support the hypothesis that the piriformis plays a stabilizing role during bipedal progression.

Assuming the relative width of the caudal sacral elements relates to the size and strength of the piriformis muscle, it would be expected that bipedal primates would have wide caudal sacral elements and arboreal/quadrupedal primates would have narrow caudal sacral elements. This expectation was confirmed by comparisons of *H. sapiens* and other hominoid caudal sacral element percentages with p-values all less than 0.05 and comparisons of nonhuman hominoid caudal sacral element percentages with almost no significant p-values. AL-288-1, *Australopithecus afarensis*, seems to exhibit a combination of these two groups by having very wide S1-S3, similar to humans, but with an S5 that is similar to nonhuman hominoids. The S4 of AL-288-1 is intermediate to these two groups. This would imply that AL-288-1 did not yet possess the derived bipedal condition of having a shorter lever arm associated with the piriformis muscle, or perhaps lacked the need for the stabilizing action of the piriformis.

Conclusion

Among extant hominoids, there is a strong relationship between auricular surface and acetabular diameter and between sacral body and acetabular diameter. However, the auricular surface area of the sacroiliac joint has greater variability than do acetabular and sacral body joint sizes, and should be further examined. The variation observed in this joint could be partially attributed to the change in the surface morphology of this joint throughout the lifetime of an individual and the "interlocking" nature of this joint. The nature of this joint has not been sufficiently

explored in nonhuman primates and could play a similar role in force distribution to the role it plays in humans.

The findings of this study corroborate previous studies that have found that an increase in acetabular diameter preceded an increase in first sacral body area (Jungers, 1988) during the course of hominin evolution. This implies a gradual shift in locomotor modes during the hominin lineage, as shown by the fossils included in this study (AL-288-1, Sts 14, STW 431, BSN49/P27, KNM-ER 3228, and SH1). In both auricular surface area and sacral body area there was a larger range of variation than seen in acetabular diameter, possibly due to the plastic nature of these joints. Ligamentous structures around the joint likely play a large role in mitigating force through these joints, particularly the auricular surface, and should be examined comparatively across primates to understand the effects that potential force dissipating structures, such as ligamentous reinforcement, may play in these joint complexes.

This study found that *Homo sapiens*, but not other hominoids, have caudally as well as cranially wide sacral vertebrae, which would result in a shortened piriformis muscle in modern humans. This could allow for faster action of this muscle and stability of the torso in upright walking, a theory that should be investigated in future studies.

Works Cited

Abitbol MM. 1987. Evolution of the sacrum in hominoids. *American Journal of Physical Anthropology* 74:65-81.

Aiello L and Dean C. 1990. An introduction to human evolutionary anatomy. Academic press.

Ankel-Simons F. 2000. Primate Anatomy. New York: Academic press.

Arsuaga JL, Lorenzo C, Carretero JM, Gracia A, Martinez I, Garcia N, Bermudez de Castro JM, Carbonell E. 1999. A complete human pelvis from the Middle Pleistocene of Spain. *Nature* 399:255-258.

Auerbach BM and Ruff CB. 2004. Human body mass estimation: a comparison of "morphometric" and "mechanical" methods. *American journal of physical anthropology* 125:331-342.

Berge C. 1991. Size- and locomotion-related aspects of hominid and anthropoid pelves: an osteometrical multivariate analysis. In: Jouffroy FK, Stack MH, and Niemitz C, editors. Gravity, Posture, and Locomotion in primates. Il Florence: Sedicesimo. p96-108.

Berge C and Kazmierczak JB. 1986. Effects of size and locomotor adaptations on the hominid pelvis: evaluation of australopithecine bipedality with a new multivariate method. *Folia primatologica* 46:185-204.

Bischoff JL, Shamp DD, Aramburu A, Arsuaga JL, Carbonell E, Bermudez de Castro JM. 2003. The Sima de los Huesos Hominids date to beyond U/Th Equilibrium

(>350kyr) and perhaps to 400-500 kyr: New Radiometric dates. *Journal of Archaeological Science* 30:275-280.

Bonmati A, Gomez-Olivencia A, Arsuaga JL, Carretero JM, Gracia A, Martinez I, Lorenzo C, Bermudez de Castro JM, Carbonell E. 2010. Middle Pleistocene lower back and pelvis from an aged human individual from the Sima de los Huesos site, Spain. *PNAS* 107:18386-18391.

Bowen V and Cassidy DJ. 1981. Macroscopic and microscopic anatomy of the sacroiliac joint from embryonic life until the eighth decade. *Spine* 6:620-628.

Bramble DM and Lieberman DE. 2004. Endurance running and the evolution of *Homo*. *Nature* 432:345.

Brown F, Harris J, Leakey R, Walker A. 1983. Early *Homo erectus* skeleton from west Lake Turkana, Kenya. *Nature* 316:788-792.

Cheng JS and Song JK. 2003. Anatomy of the sacrum. *Neurosurgical focus* 15:2.

Correa TA, Corssley KM, Kim HJ, and Pandy MG. 2010. Contributions of individual muscles to hip joint contact force in normal walking. *Journal of Biomechanics* 43:1618-1622.

Filler AG. 1994. Evolution of the sacrum in hominids. In: Doty JR, Rengachary SS (Eds.), Surgical disorders of the sacrum. Thieme: New York. 13-20.

Giphart JE, Stull JD, LaPrade RF, Wahoff MS, Philippon MJ. 2012. Recruitment and activity of the pectineus and piriformis muscles during hip rehabilitation exercises. *The American Journal of Sports Medicine* 40:1654-1663.

Grieve EFJ. 1983. Mechanical dysfunction of the sacroiliac joint. *International Rehabilitation Medicine* 5:46-52.

Haeusler M. 2002. New Insights into the locomotion of Australopithecus africanus based on the pelvis. *Evolutionary Anthropology* S1:53-57.

Haile-Selassie Y, Latimer BM, Alene M, Deino AL, Gilbert L, Melillo SM, Saylor BZ, Scott GR, and Lovejoy CO. 2010. An early *Australopithecus afarensis* postcranium from Woranso-Mille, Ethiopia. *PNAS* 107: 12121-12126.

Jenkins FA and Camazine SM. 1977. Hip structure and locomotion in ambulatory and cursorial carnivorans. *J. Zoo. Lond*. 181:351-370.

Johanson DC, Masao FT, Eck GG, White TD, Walter RC, Kimbel WH, Asfaw B, Manega P, Nolessokia P, and Suwa G. 1987. New Partial skeleton of *Homo habilis* from Olduvai Gorge, Tanzania. *Nature* 327:205-209.

Jungers WJ. 1988. Relative joint size and hominoid locomotor adaptations with implications for the evolution of hominid bipedalism. *Journal of Human Evolution* 17:247-265.

Jungers WL. 1991. Scaling of postcranial joint size in hominoid primates. In: Jouffroy FK, Stack MH, and Niemitz C (Eds.), Gravity, Posture, and Locomotion in primates. Il Sedicesimo: Florence. 87-95.

Kibii JM, Churchill SE, Schmid P, Carlson KJ, Reed ND, de Ruiter DJ, and Berger LR. 2011. A partial pelvis of *Australopithecus sediba*. *Science* 333, 1407.

Kimbel WH, Johanson DC, Rak J. 1994. The first skull and other new discoveries of *Australopithecus afarensis* at Hadar, Ethiopia. *Nature* 368:449-451.

Leutenegger W. 1972. Newborn size and pelvic dimensions of *Australopithecus*. *Nature* 240:568-569.

Leutenegger W. 1974. Functional aspects of pelvic morphology in simian primates. *Journal of human Evolution* 3:207-222.

Leutenegger W. 1977. A functional interpretation of the sacrum of *Australopithecus africanus*. *South African Journal of Science* 73:308-310.

Lewton KL. 2010. Locomotor function and evolution of the primate pelvis [Ph.D.] Tempe: Arizona State University

Lieberman DE, Devlin MJ, Pearson OM. 2001. Articular area responses to mechanical loading: effects of exercise, age, and skeletal location. *American journal of physical anthropology* 116:266-277.

Lordkipanidze D, Jashashvili T, Vekua A, Ponce de Leon MS, Zollikofer CPE, Rightmire GP, Pontzer H, Ferring R, Oms O, Tappen M, Bukhsianidze M, Agusti J, Kahlke R, Kiladze G, Martinez-Navarro B, Mouskhelishvili A, Nioradze M, Rook L. 2007. Postcranial evidence from early *Homo* from Dmanisi, Georgia. *Nature* 449:305-310.

Lovejoy CO. 1978. A biomechanical review of the locomotor diversity of early hominids. Early hominids of Africa 403:429.

Lovejoy CO. 1988. Evolution of human walking. *Scientific American* 259:118-125.

Lovejoy CO. 2005a. The natural history of human gait and posture, part 1, spine and pelvis. *Gait & Posture* 21:95-112.

Lovejoy CO. 2005b. The natural history of human gait and posture, part 2, hip and thigh. *Gait & Posture* 21:113-124.

Mahato NK. 2010. Variable positions of the sacral auricular surface: classification and importance. *Neurosurgical focus* 28:3.

McDonald, J.H. 2014. Handbook of Biological Statistics (3rd ed.). Sparky House Publishing, Baltimore, Maryland.

McHenry HM. 1986. The first bipeds: a comparison of the *A. afarensis* and *A. africanus* postcranium and implications for the evolution of bipedalism. *Journal of human evolution* 15:177-191.

McHenry HM. 1991. First steps? Analyses of the postcranium of early hominids. In: Origine(s) de la Bipédie Chez les hominidés, Y. Coppens, B. Senut, editors. Paris: Editions du CNRS. p. 133-141.

McHenry HM. 1992. Body size and proportions in early hominids. *American Journal of Physical Anthropology* 87:407-431.

Michaud T. 2012. Strength and stress fractures. *Dynamic Chiropractic* 5:2.

Pal GP. 1989. Weight transmission through the sacrum in man. *Journal of Anatomy* 162:9-17.

Pal GP and Routal RV. 1987. Transmission of weight through the lower thoracic and lumbar region of the vertebral column in man. *Journal of Anatomy* 152:93-105.

Robinson JT. 1972. Early hominid posture and locomotion. University of Chicago Press, Chicago.

Rose M. 1984. A hominine hip bone, KNM-ER 3228, from East Lake Turkana, Kenya. *American Journal of Physical Anthropology* 63:371-378.

Ruff C. 1988. Hindlimb articular surface allometry in Hominoidea and Macaca, with comparisons to diaphyseal scaling. *Journal of Human Evolution* 17: 687-714.

Ruff CB. 1991. Climate and body shape in hominid evolution. *Journal of Human Evolution* 21:81-105.

Ruff CB. 2003. Long bone articular and diaphyseal structure in Old World monkeys and apes. II: Estimation of body mass. *American Journal of Physical Anthropology* 120:16-37.

Ruff C. 2010. Body size and body shape in early hominins – implications of the Gona Pelvis. *Journal of Human Evolution* 58:166-178.

Ruff CB, Walker A, Teaford MF. 1989. Body mass, sexual dimorphism and femoral proportions of *Proconsul* from Rusinga and Mfangano Islands, Kenya. *Journal of Human Evolution* 18:515-536.

Ruff CB, Scott WW, Liu AYC. 1991. Articular and diaphyseal remodeling of the proximal femur with changes in body mass in adults. *American Journal of Physical Anthropology* 86:397-413.

Ruff CB and Walker A, 1993. Body size and body shape. In: *The Nariokotome* Homo erectus *skeleton*, A. Walker, R. Leakey, editors. Cambridge: Harvard University press. p. 234-265.

Ruff CB, Trinkaus E, Holliday TW. 1997. Body mass and encephalization in Pleistocene Homo. *Nature* 387:173-176.

Sanders WJ. 1995. Function, allometry, and evolution of the Australopithecine lower precaudal spine [Ph.D.] New York: New York University.

Simonian PT, Routt MLC, Harrington RM. 1994. Biomechanical simulation of the anteroposterior compression injury of the pelvis. *Clinical orthopaedics and related research* 309:245-256.

Simpson SW, Quade J, Levin NE, Butler R, Dupont-Nivet G, Everett M, and Semaw S. 2008. A female *Homo erectus* pelvis from Gona, Ethiopia. *Science* 322:1089-1092.

Simpson SW, Quade J, Levin NE, Semaw S. 2014. The female Homo pelvis from Gona: Response to Ruff (2010). *Journal of Human Evoluion* 68:32-35.

Smith RJ and Junger WL. 1997. Body mass in comparative primatology. *Journal of human evolution* 32:523-559.

Snijders CJ, Ribbers MTLM, de Bakker HV, Stoeckart R, Stam HJ. 1998. EMG recordings of abdominal and back muscles in various standing postures: validation of biomechanical model on sacroiliac joint stability. *Journal of Electromyography and Kinesiology* 8:205-214.

Stern JT and Susman RL. 1983. The locomotor anatomy of Australopithecus afarensis. *American Journal of Physical Anthropology* 60:279-317.

Swartz SM. 1989. The functional morphology of weight bearing: limb joint surface area allometry in anthropoid primates. *Journal of Zoology, London* 218:441-460.

Tague RB and Lovejoy CO. 1986. The obstetric pelvis of A.L. 288-1 (Lucy). *Journal of Human Evolution* 15: 237-255.

Tobias PV. 1987. 21st Annual Report of PARU and its Precursors. Department of Anatomy, University of Witwatersrand, Johannesburg.

Toussaint M, Macho GA, Tobias PV, Partridge TC, and Hughes AR. 2003. The third partial skeleton of a late Pliocene hominin Stw 431 from Sterkfontein, South Africa. *South African Journal of Science* 99:215-223.

Vleeming A, Volkers ACW, Snijders CJ, Stoeckart R. 1990. Relation between form and function in the sacroiliac joint 2:Biomechanical aspects. *Spine* 15:130-132.

Vleeming A, Stoeckart R. 2007. Movement, stability, and lumbopelvic pain, eds Vleeming et al. London: Churchill Livingstone. P 113-140.

Walker A, Ruff CB. 1993. The reconstruction of the pelvis. In: *The nariokotome* Homo erectus *skeleton*, A. Walker, R. Leakey, editors. Cambridge: Harvard University press. p. 221-233.

Ward CV. 1991. Functional anatomy of the lower back and pelvic of the Miocene hominoid *Proconsul nyanzae* from Mfango Island, Kenya [Ph.D.]. Baltimore: Johns Hopkins University.

Ward CV, Feibel CS, Hammond AS, Leakey LN, Moffett EA, Plavcan JM, Skinner MM, Spoor F, and Leakey MG. 2015. Associated ilium and femur from Koobi Fora, Kenya, and postcranial diversity in early *Homo*. *Journal of Human Evolution*. In press.

Willard FH. 2007. Movement, stability, and lumbopelvic pain. Vleeming et al. editors.

London: Churchill Livingstone. p. 5-46.